Supporting information for "High-efficiently reclaiming phosphate from an aqueous solution by bentonite modified biochars: a slow release fertilizer with a precise rate regulation"

Xiongfang An[1], Zhansheng Wu[1, 2]*, Junzhi Yu[1], Linhan Ge[4], Tao Li[1], Xiaochen Liu[2] and Bing Yu[3]*

1. School of Chemistry and Chemical Engineering/Key Lab. for Green Processing of Chemical Engineering of Xinjiang Bingtuan, Shihezi University, Shihezi 832003, P.R. China.

2. School of Environmental and Chemical Engineering, Xi'an Polytechnic University, Xi'an 710048, P.R. China.

3. Fujian Key Laboratory of Pollution Control and Resource Reuse, School of Environmental Science and Engineering, Fujian Normal University, Fuzhou 350007, Fujian Province, China

4. Discipline of Chemical Engineering, School of Engineering, University of Newcastle, 2308, Australia.

Corresponding author: Zhansheng Wu,

Tel: +86 029-62779279, Fax: +86029-62779281

Email address: wuzhans@126.com

Corresponding author: Bing Yu, Tel: +86 18850405140, Email address: bing.yu@uon.edu.au

Supporting Information: Pages: 20, Figures: 11, Tables: 10.

Table of Contents **Page**

Eleven figures

Eight tables

2.1. Kinetics of thermal degradation

The yield of BSRFs (Y) and the volatilisation rate of CS (V) in BSRFs were calculated using the following equations [1-3]:

$$\boldsymbol{Y = \frac{M_1}{M_2} \times 100\%} \quad (1)$$

$$\boldsymbol{V = 1 - \frac{M_1 - M_3}{M_4} \times 100\%} \quad (2)$$

where, M_1, M_2, M_3 and M_4 represent the weights of obtained BSRFs, bentonite-CS composites, bentonite and CS, respectively [4].

The pyrolytic process of biomass can be represented by the following reaction scheme:

$$\text{A (biomass)} \rightarrow \text{B (biochar)} + \text{C (gas)}, \ \Delta H = ? \text{ kJ/mol} \quad (3)$$

According to Arrhenius equation, k(T) is usually expressed as follows:

$$k(T) = A \exp\left(-\frac{E}{RT}\right) \quad (4)$$

The conversion (α) is expressed as:

$$\alpha = \frac{m_o - m_t}{m_o - m_\infty} \quad (5)$$

Where m_o is the initial mass of the sample, m_t is the mass of sample at the time of t, and m_∞ is the final indecomposable mass of the sample in the pyrolysis process.

The heating rate β(K/s)

$$\beta = \frac{dT}{dt} \quad (6)$$

Flynn-Wall-Ozawa (FWO), Kissinger-Akahira-Sunose (KAS) and Starink models (STK) are applied for the determination of the apparent activation energy (E_α) in this work. It is well known that the conversional method provides feasible methods for the estimation of E_α because of their good adaptability and validity for model-free approaches[5, 6].

FWO: $$\ln\beta = \ln\left[\frac{0.0048AE_\alpha}{RG(\alpha)}\right] - 1.0516\frac{E_\alpha}{RT} \quad (7)$$

KAS: $$\ln\frac{\beta}{T^2} = \ln\left[\frac{AR}{E_\alpha G(\alpha)}\right] - \frac{E_\alpha}{RT} \quad (8)$$

Starink: $$\ln\frac{\beta}{T^{1.8}} = C_S - 1.0037\frac{E_\alpha}{RT} \quad (9)$$

At a constant conversion rate α, the plots of ln (β) versus 1/T (FWO), ln (β/T_α^2) versus $1/T$ (KAS) and ln ($\beta/T_\alpha^{1.8}$) versus $1/T$ (SKM) obtained from TG plots, the slopes of the straight lines can be used to determine the apparent activation energy.

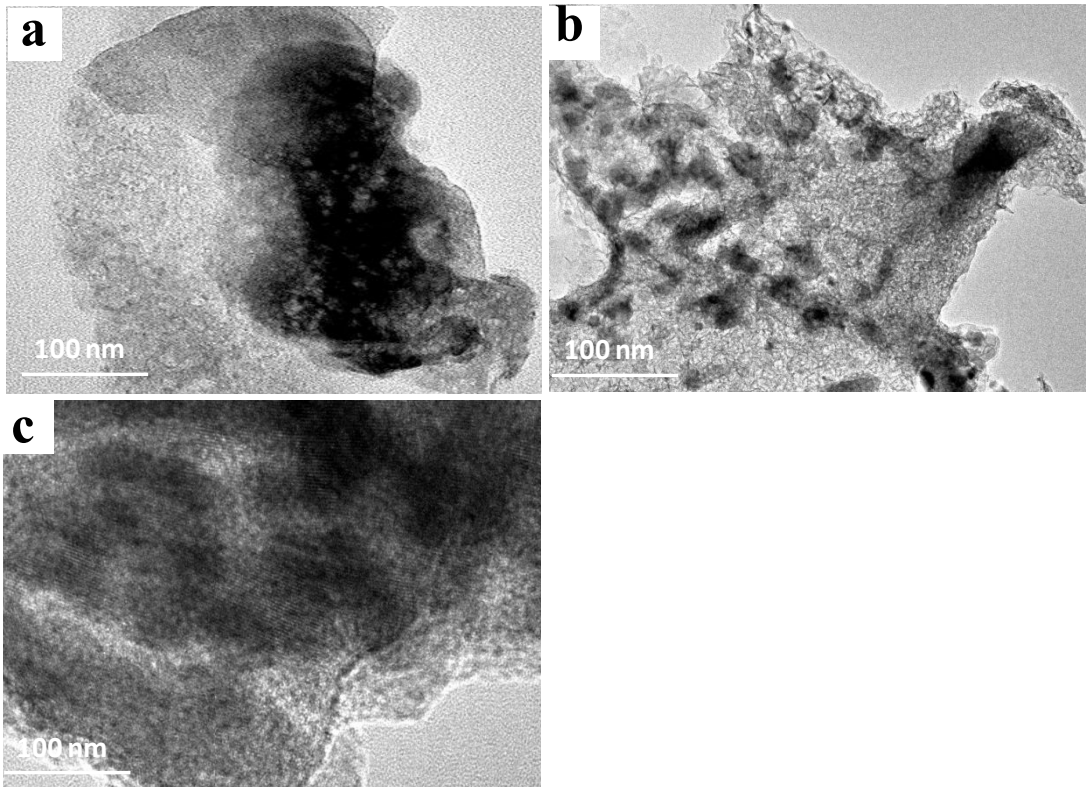

Figure S1 The low-magnification TEM images of a) H-BSRF, b) N-BSRF and c) OH-BSRF.

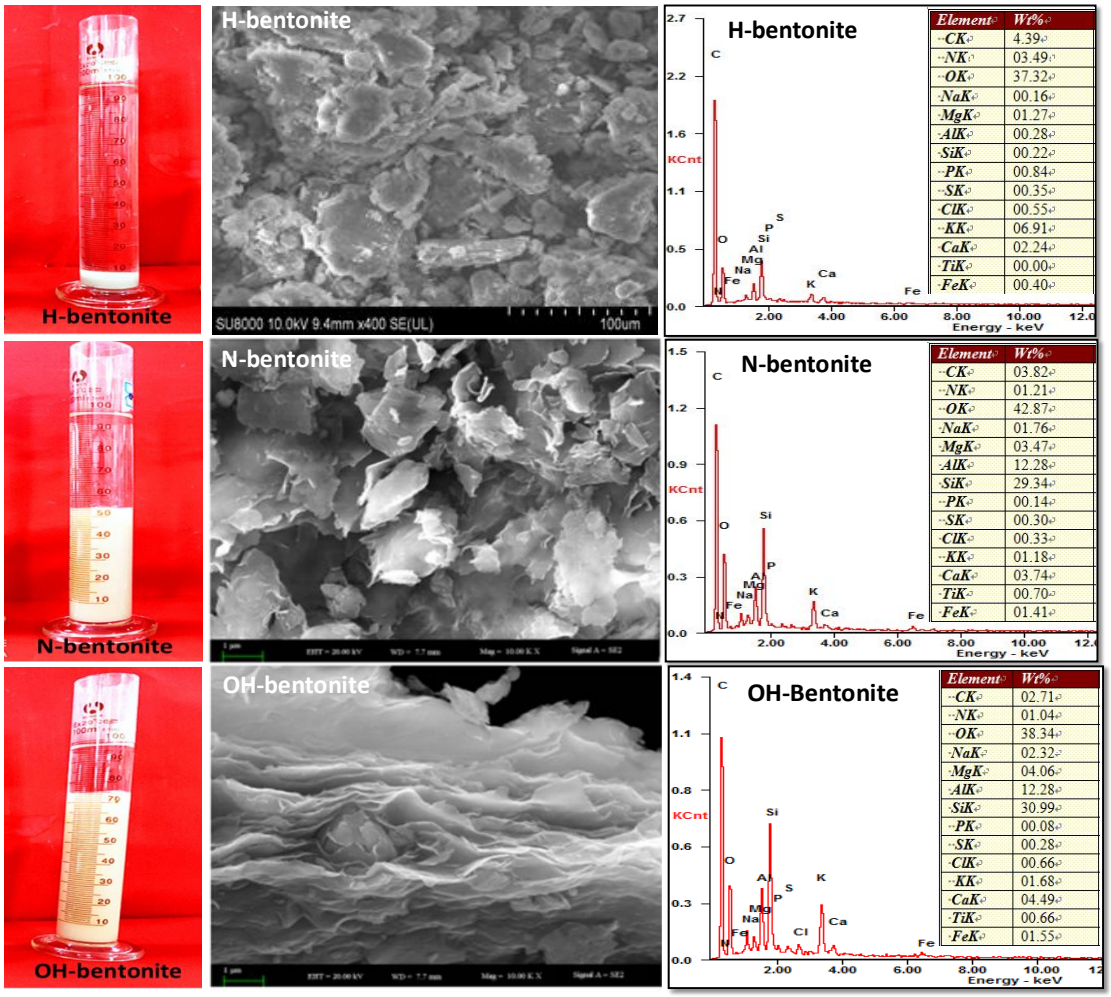

Figure S2 The swell abilities and SEM-EDS images for H-bentonite, N-bentonite and OH-bentonite.

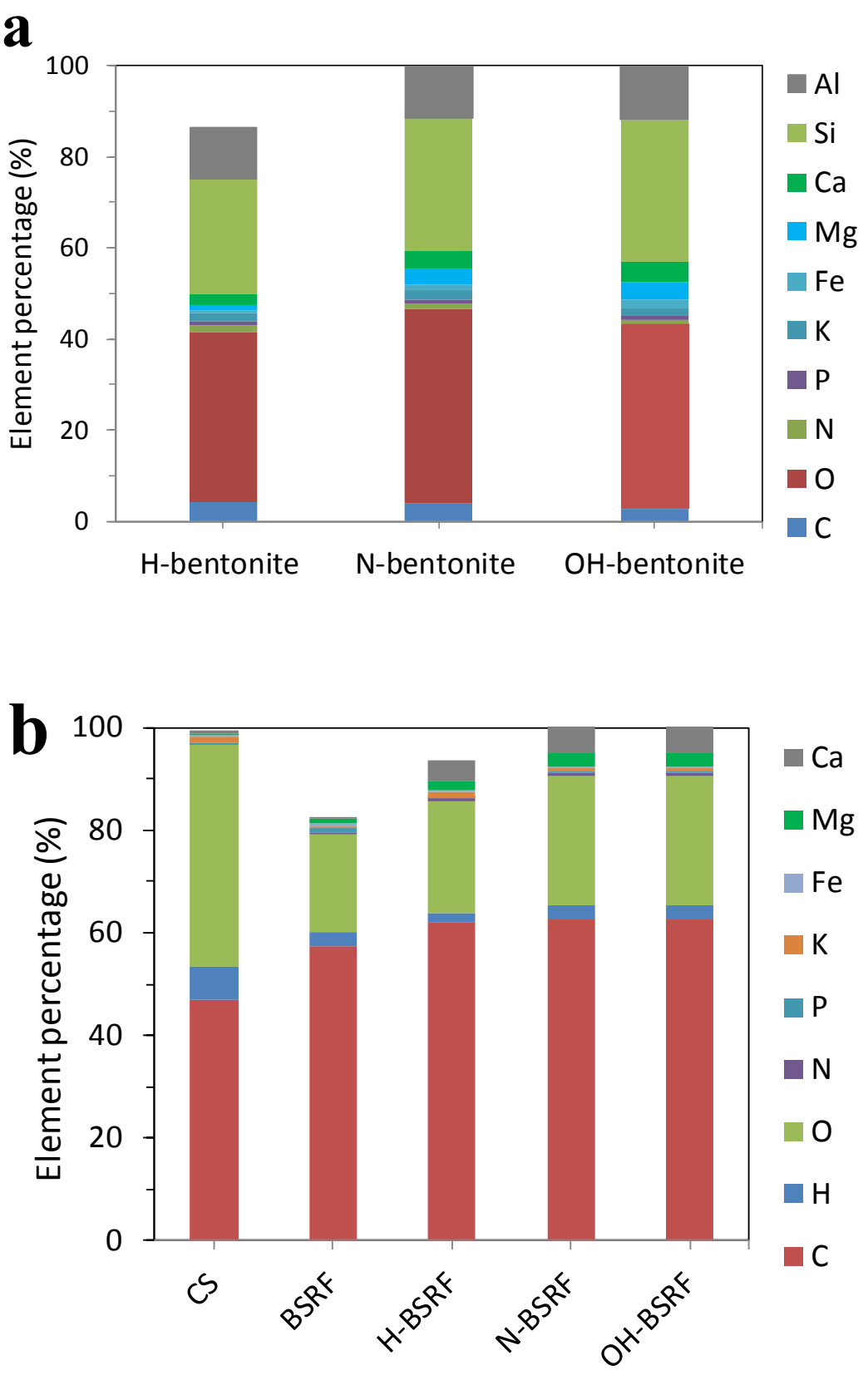

Figure S3 ICP elemental analysis of various modified bentonites and BSRF.

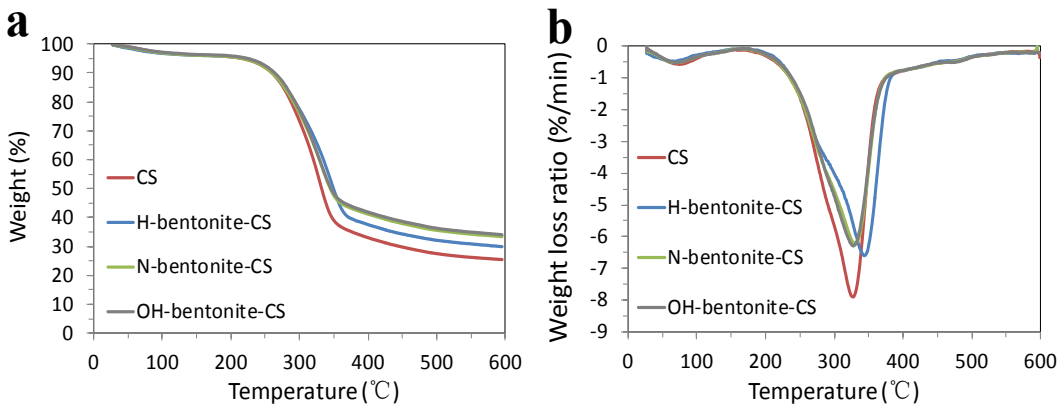

Figure S4 TG-DSC curves of CS, H-bentonite-CS composite, N-bentonite-CS composite and OH-bentonite-CS composite at β = 10 °C/min.

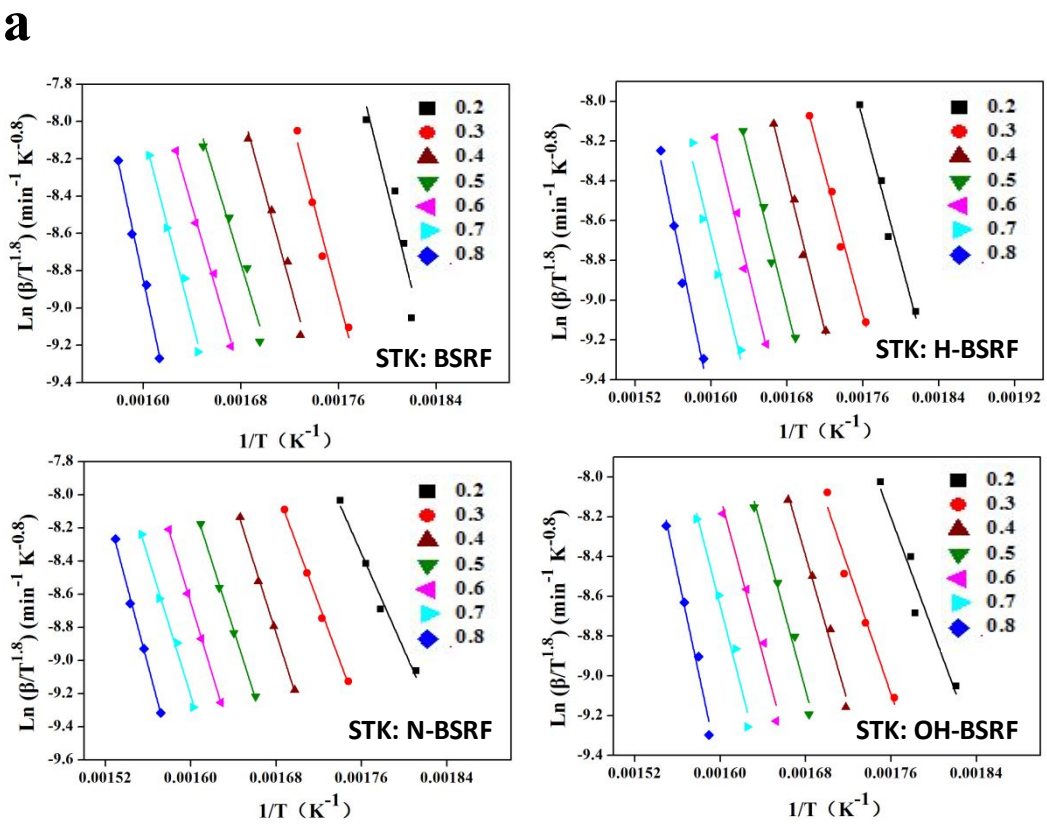

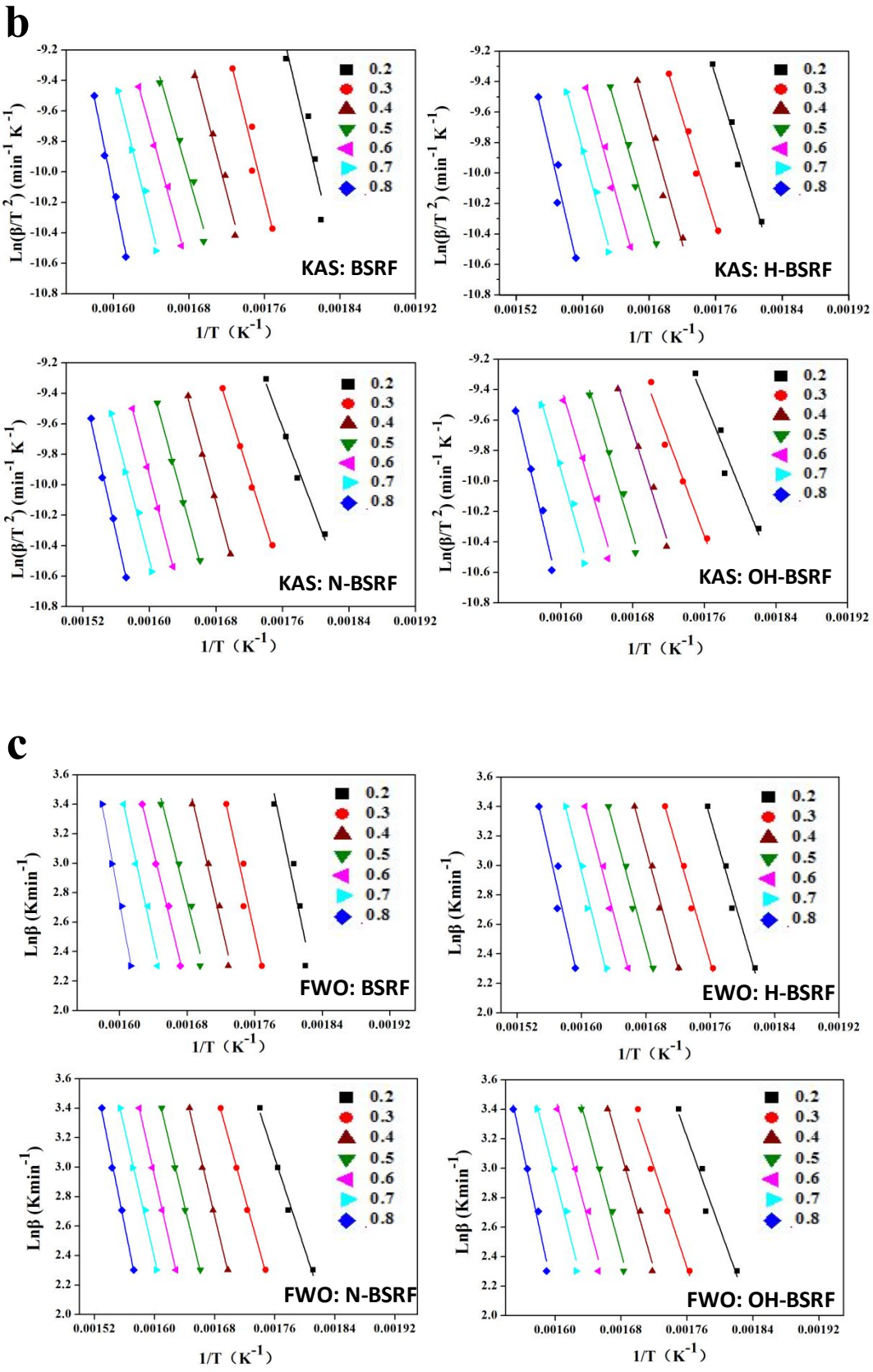

Figure S5 Linear fitting a) Starink, b) Kissinger-Akhira-Sunose and c) Flynn-Wall-Ozawa.

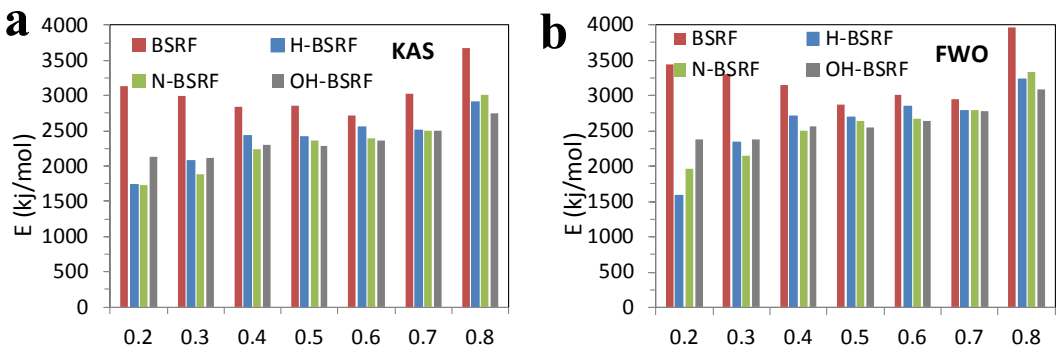

Figure S6 The activation energies of various BSRFs at different yield ratios under the KAS and FWO.

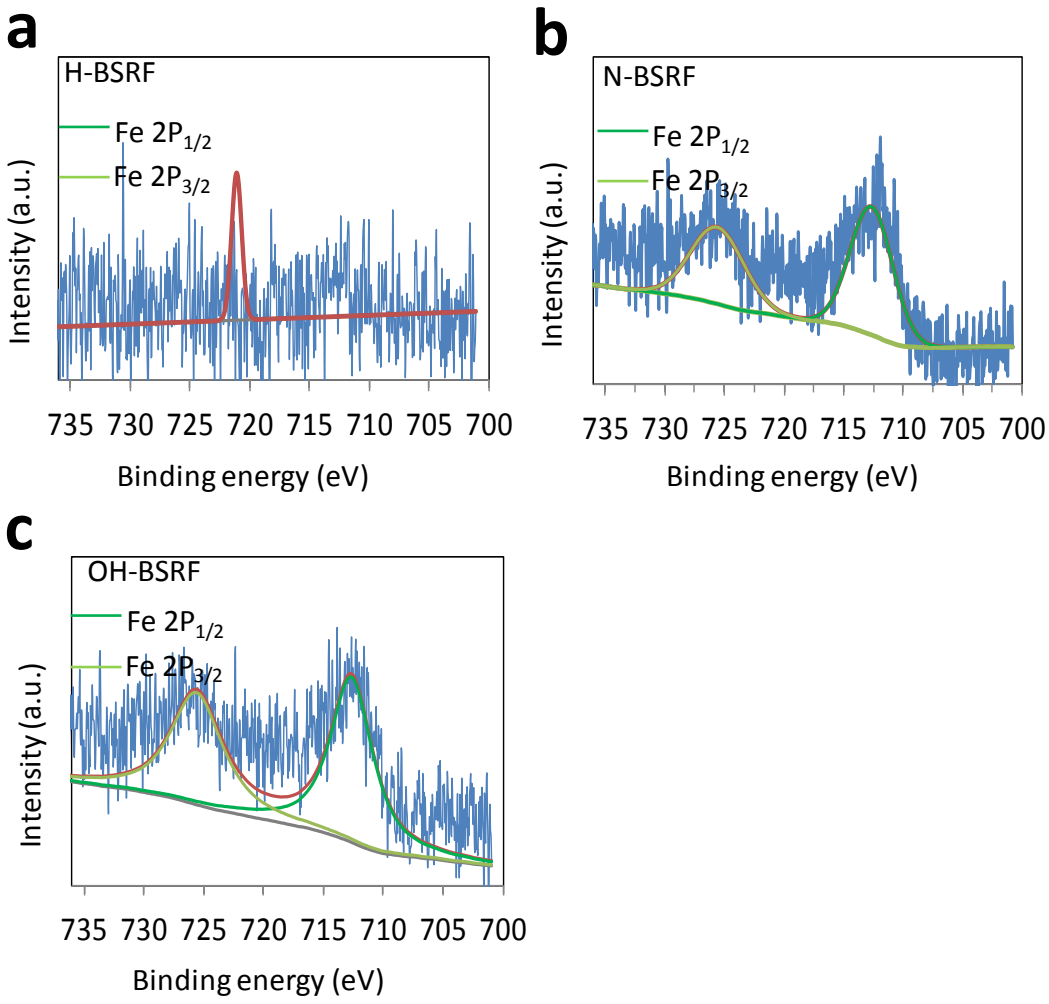

Figure S7 XPS analysis of Fe related speciation.

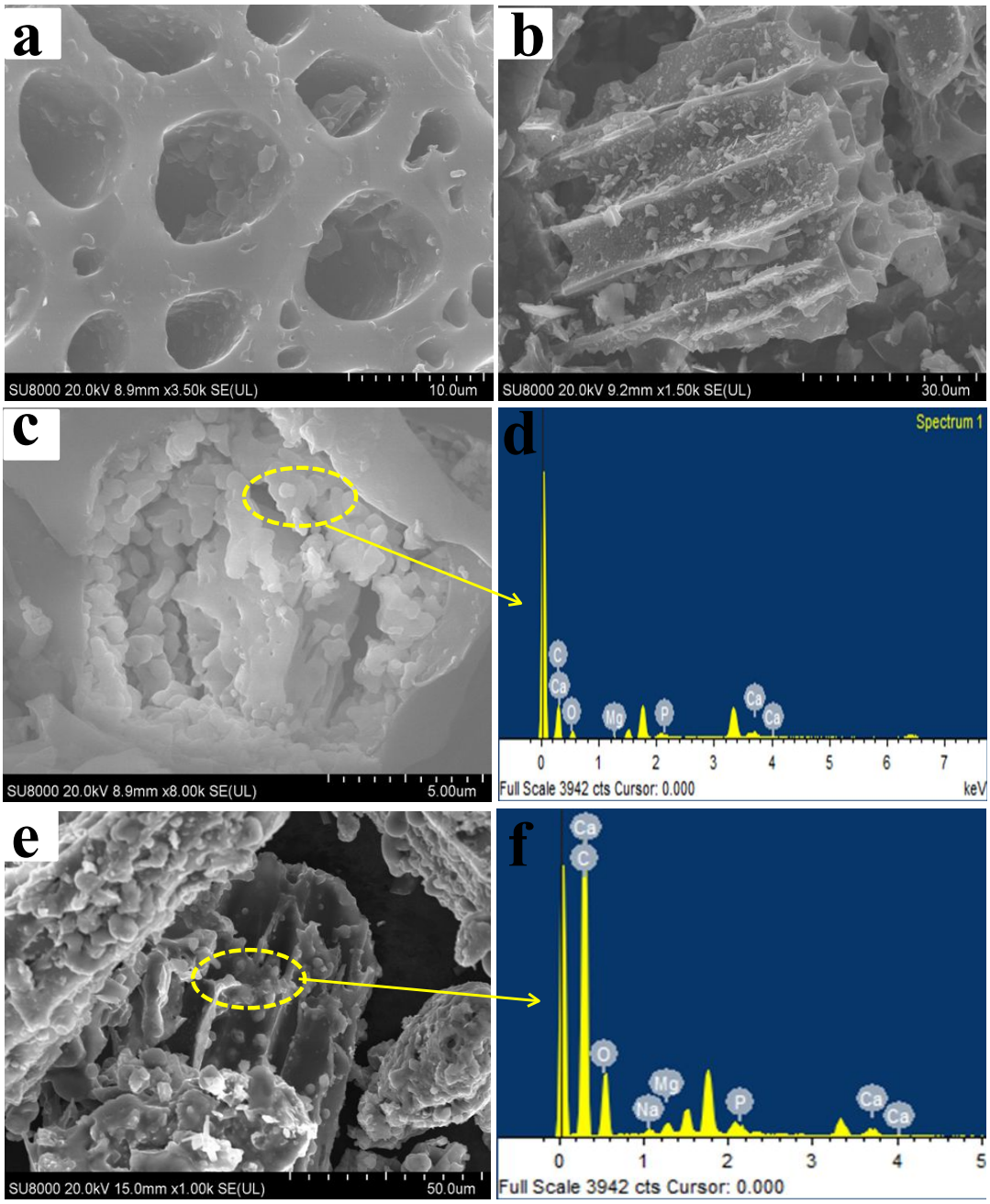

Figure S8 SEM-EDX a) P-loaded BSRF, b) P-loaded H-BSRF, c and d) P-loaded N-BSRF, and e and f) P-loaded OH-BSRF morphological structures and element distribution.

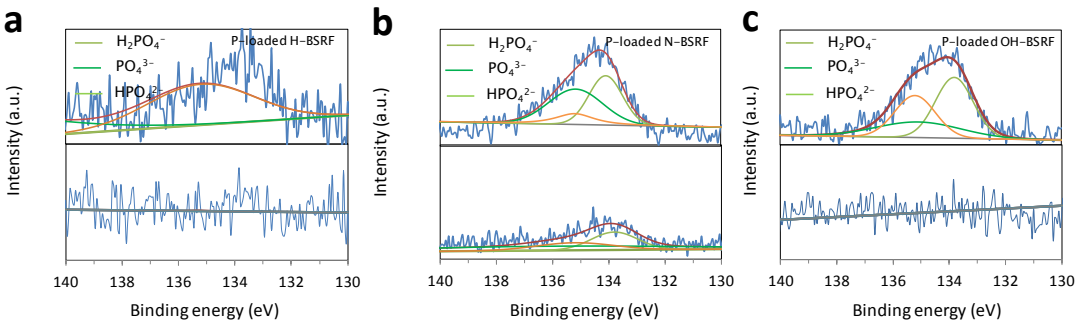

Figure S9 XPS spectra of P 2p for a) H-BSRF, b) N-BSRF, and c) OH-BSRF before and after phosphate adsorption.

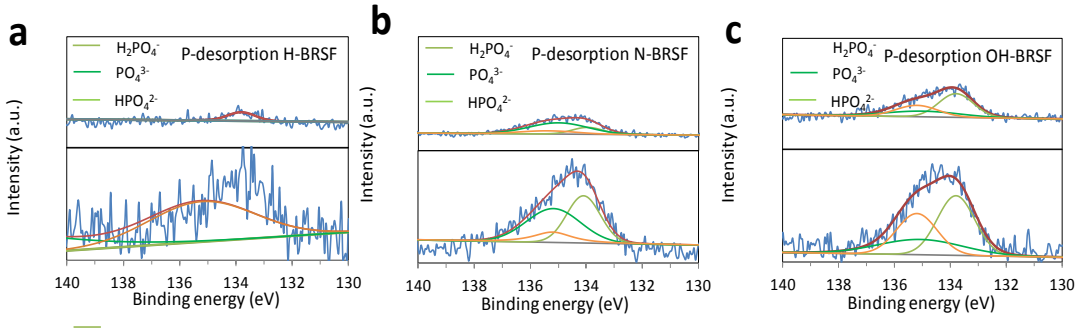

Figure S10 XPS spectra of P 2p for a) H-BSRF, b) N-BSRF, and c) OH-BSRF before and after P desorption.

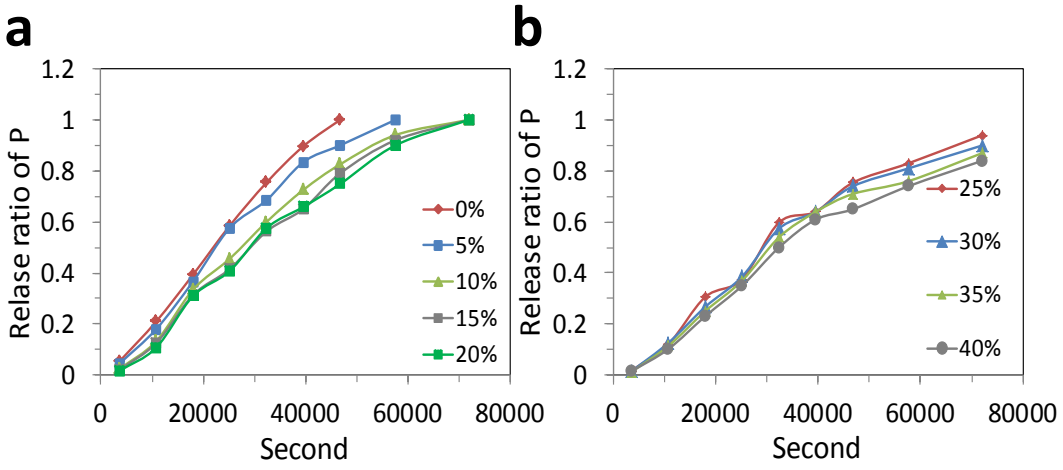

Figure S11 a) P release performance from OH-BSRFs with different contents of OH-bentonite ranging from 0 to 20% for establishing a modified Fick model; and b) the experimental verification for P release performance from OH-BSRFs with different contents of OH-bentonite ranging from 25 to 40%.

Table S1 Basic physical properties of modified bentonites

Sample	H-Bent	Na-Bent	OH-Bent
Montmorillonite (%)	42	78	65
Swellability (ml/g)	63.0	84.0	6.5
Gum price (ml/15g)	157.51	855.42	870.27
EC (ms/cm)	6.76	3.17	2.22
pH	2.81	10.06	10.17
CEC (mol/kg)	13.56	25.78	15.61
BET (m^2/g)	6.58	10.03	16.79
PV (cm^3/g)	0.041	0.067	0.075
PS(Å)	249.25	268.28	223.48

Table S2 Basic physical and chemical characteristics of the used soil

pH	8.16	EC (us/cm)	688
Total N (g/kg)	0.91	Available N (g/kg)	0.13
Total P(g/kg)	1.06	Available P (g/kg)	0.69
Total K(g/kg)	22.58	Available K (g/kg)	3.63

Table S3 pH, EC, CEC, BET, surface area and production ratios of BSRFs

Samples	Production ratio (%)	pH	EC (us/cm)	BET (m^2/g)	PV (cm^3/g)	PS(nm)
CS		7.74	2.42	4.42	0.0070	10.671
BSRF	18.54	8.28	157.41	125.23	0.1140	6.332
H-BSRF	32.80	5.41	214.43	87.05	0.0584	7.827
N-BSRF	35.57	8.96	192.80	104.55	0.0756	5.793
OH-BSRF	36.15	9.20	172.52	134.06	0.0886	4.227

Table S4 Adsorption capacity of phosphate of various reported biochars

Biochars	Adsorption condition (mg/L, °C , Time and pH)	Adsorption capacity (mg/g)	References
Fe-sugar beet tailings biochar	61.5 (mg/25 °C L), , 8 to 12 h, near-neutral pH	44.53	Yao et al[8]
MgO-enriched tomato biochar	150 (mg/L), 22 °C, 24 h, near-neutral pH	100	Yao et al[7]
montmorillonite-biochar	200 (mg/L), 22 °C, 24 h, normal pH	105.28	Chen et al[3]
Wheat straw biochar	500 (mg/L), 22 °C, 18 h, near-neutral pH	109.34	Huang et al [9]
($MgFe_2O_4$)-magnetic biochar	200 (mg/L), 22 °C, 24 h, near-neutral pH	197.56	Jung et al[10]
Calcium-activated biochar	100 (mg/L), 22 °C, 24 h, near-neutral pH	197	Liu et al[11]
Mg/Alcalcined layered biochar	100 (mg/L), 22 °C, 8 h, near-neutral pH	99	Lee et al[12]
Fe/Al (Hydr)oxides-biochars	300 (mg/L), 25°C, 8 h, near-neutral pH	80	Peng et al[13]
BSRF	500 (mg/L), 25 °C, 24 h, near-neutral pH	157.18	
H-BSRF	500 (mg/L), 25 °C, 24 h, near-neutral pH	227.32	
N-BSRF	500 (mg/L), 25 °C, 24 h, near-neutral pH	233.45	This work
OH-BSRF	500 (mg/L), 25 °C, 24 h, near-neutral pH	245.56	

Table S5 Kinetic models for phosphate adsorption by BSRFs

	Samples	Parameter 1	Parameter 2	Parameter 3	R^2
Frist-order	BSRF	k=4.643	q_e=12.38		0.978
	H-BSRF	k=4.785	q_e=12.40		0.835
	N-BSRF	k=4.894	q_e=12.41		0.892
	OH-BSRF	k=5.092	q_e=12.44		0.912
Second-order	BSRF	k=10.782	q_e=13.61		0.873
	H-BSRF	k=10.864	q_e=13.64		0.923
	N-BSRF	k=10.965	q_e=13.68		0.951
	OH-BSRF	k=10.988	q_e=13.74		0.967
n_th-order	BSRF	k=4.756	q_e=12.94	n=1.021	0.9842
	H-BSRF	k=9.674	q_e=12.98	n=1.740	0.9934
	N-BSRF	k=10.178	q_e=13.14	n=1.741	0.9953
	OH-BSRF	k=10.356	q_e=13.31	n=1.742	0.9967
Elovich	BSRF	β=7.567	α=2.674		0.573
	H-BSRF	β=7.745	α=2.743		0.656
	N-BSRF	β=7.834	α=2.756		0.721
	OH-BSRF	β=7.875	α=2.934		0.756

Table S6 Kinetic study for the slow release of P from BSRFs

Kinetics models		BSRF	H-BSRF	N-BSRF	OH-BSRF
Zero-order kinetics	R_1^2	0.9252	0.9939	0.9661	0.9934
	k_1	0.0719	0.0496	0.0377	0.0408
First-order release kinetics	R_2^2	0.9738	0.9354	0.8921	0.9138
	k_2	-0.2692	-0.1587	-0.0842	-0.1127
Higuchi model	R_3^2	0.9917	0.9846	0.9963	0.9809
	k_3	0.3241	0.2614	0.2241	0.2126
Hixson-Crowell model	R_4^2	0.9252	0.9767	0.9661	0.9934
	k_4	0.0240	0.0157	0.0126	0.0136
Baker-Lonsdale model	R_5^2	0.8832	0.9930	0.8850	0.9565
	k_5	-0.0970	-0.0364	-0.0215	-0.0241

Table S7 Higuchi kinetic study for the slow release of P from OH-BSRF with different contents of OH-bentonite ranging from 0 to 20%

Samples	k	R^2
0	0.0064	0.982
5%	0.0057	0.985
10%	0.0052	0.984
15%	0.0051	0.986
20%	0.0048	0.979

Table S8 The surface area (BET), pore size (PS) and pore volume (PV) of OH-BSRFs with different contents of OH-bentonite ranging from 0 to 40%

Samples	BET (m^2/g)	PV (cm^3/g)	PS (nm)
0	56.59	0.1144	6.332
5%	82.76	0.1085	5.242
10%	98.13	0.1144	4.663
15%	134.45	0.1442	4.227
20%	146.51	0.1303	4.190
25%	147.68	0.8389	3.898
30%	157.56	0.1199	3.853
35%	169.07	0.1534	3.488
40%	188.41	0.1409	2.991

Table S9 The diffusion coefficient *D* of OH-BSRF with different contents of OH-bentonite ranging from 0 to 40%

Samples (OH-BSRF)	*D* (water system cm^2/s)	*f* (blocking coefficient)	*k* (predicated value)
0	45.2	3.5 × 10^7	0.0064
5%	45.2	3.5 × 10^7	0.0058
10%	45.2	3.5 × 10^7	0.0054
15%	45.2	3.5 × 10^7	0.0052
20%	45.2	3.5 × 10^7	0.0051
25%	45.2	3.5 × 10^7	0.0049
30%	45.2	3.5 × 10^7	0.0049
35%	45.2	3.5 × 10^7	0.0047
40%	45.2	3.5 × 10^7	0.0043

Table S10 Higuchi kinetic study for the slow release of P from OH-BSRF with different contents of OH-BSRF ranging from 25 to 40%

Samples	*k* (real)	R^2
25%	0.0049	0.976
30%	0.0048	0.979
35%	0.0046	0.975
40%	0.0044	0.976

References

1. Zheng, Y.; Wang, B.; Wester, A. E.; Chen, J.; He, F.; Chen, H.; Gao, B., Reclaiming phosphorus from secondary treated municipal wastewater with engineered biochar. *Chem. Eng. J.***2019,** *362*, 460-468. DOI:10.1016/j.cej.2019.01.036

2 Chen, Q.; Qin, J.; Sun, P.; Cheng, Z.; Shen, G., Cow dung-derived engineered biochar for reclaiming phosphate from aqueous solution and its validation as slow-release fertilizer in soil-crop system. *J. Clean. Prod.* **2018,** *172*, 2009-2018. DOI:10.1016/j.jclepro.2017.11.224

3. Chen, L.; Chen, X. L.; Zhou, C. H.; Yang, H. M.; Ji, S. F.; Tong, D. S.; Zhong, Z. K.; Yu, W. H.; Chu, M. Q., Environmental-friendly montmorillonite-biochar composites: Facile production and tunable adsorption-release of ammonium and phosphate. *J. Clean. Prod.* **2017,** *156*, 648-659. DOI:10.1016/j.jclepro.2017.04.050

4. Yuan, T., Tahmasebi, A., Yu, J., Comparative study on pyrolysis of lignocellulosic and algal biomass using a thermogravimetric and a fixed-bed reactor. *Bioresour. Technol* **2015,** 175, 333-341. DOI:10.1016/j.biortech.2014.10.108

5. Popescu C. Integral method to analyze the kinetics of heterogeneous reactions under non-isothermal conditions a variant on the Ozawa-Flynn-Wall method. Thermochim. Acta, **1996**, 285(2): 309-323. DOI:10.1016/0040-6031(96)02916-4

6. Sbirrazzuoli, N., Girault, Y., & Elégant, L., Simulations for evaluation of kinetic methods in differential scanning calorimetry. Part 3—Peak maximum evolution methods and isoconversional methods. *Thermochim. Acta*, **1997**.293, 25-37. DOI:org/10.1016/S0040-6031(97)00023-3

7. Yao, Y.; Gao, B.; Chen, J.; Yang, L., Engineered biochar reclaiming phosphate from aqueous solutions: mechanisms and potential application as a slow-release fertilizer. *Environ. Sci. Technol.* **2013,** *47*, (15), 8700-8708. DOI:10.1021/es4012977

8 Yao, Y.; Gao, B.; Fang J., Zhang M., Chen H., Zhou Y., Anne E. C., Sun Y., Yang L., Characterization and environmental applications of clay–biochar composites. *Chem. Eng. J.,* **2014**, *242*, 136-143. DOI:org/10.1016/j.cej.2013.12.062

9. Huang, Y., Lee, X., Grattieri, M., Yuan, M., Cai, R., Macazo, F. C., Minteer, S. D., Modified biochar for phosphate adsorption in environmentally relevant conditions. Chem. Eng. J. **2020**, 380, 375，1-12. DOI:10.1016/j.cej.2019.122375

10. Jung, K., Lee S., Lee Y. J., Synthesis of novel magnesium ferrite ($MgFe_2O_4$)/biochar magnetic composites and its adsorption behavior for phosphate in aqueous solutions. Bioresour. Technol. **2017**, 245, 751 ， 1-9. DOI:10.1016/j.biortech.2017.09.035

11. Liu, X., Shen, F., Smith Jr, R. L., Qi, X., Black liquor-derived calcium-activated biochar for recovery of phosphate from aqueous solutions. *Bioresour. Technol.* **2019**, *294*, 122-198. DOI:10.1016/j.biortech.2019.122198

12. Lee, S. Y., Choi, J. W., Song, K. G., Choi, K., Lee, Y. J., Jung, K. W., Adsorption and mechanistic study for phosphate removal by rice husk-derived biochar functionalized with Mg/Al-calcined layered double hydroxides via co-pyrolysis. *Compos. Part B- Eng*, **2019**,*176*, 107209, 1-15. DOI:10.1016/j.compositesb.2019.107209

13. Peng, Y., Sun, Y., Sun, R., Zhou, Y., Tsang, D. C., Chen, Q., Optimizing the synthesis of Fe/Al (Hydr) oxides-biochars to maximize phosphate removal via response surface model. *J. Clean. Prod.* 2**019**, 237, 117. DOI:10.1016/j.jclepro.2019.117770